metrology

MDPI

Article

Uncertainty in Dimensional Measurements During Open-Die Forging †

Marco Tarabini

Department of Mechanical Engineering, Politecnico di Milano, 20156 Milan, Italy; marco.tarabini@polimi.it

† This paper is an extension version of the conference paper: Tarabini, M. Red Hot Steel: Challenges of 3D Optical Metrology in Open-Die Forging. In Proceedings of the International Archives of the Photogrammetry, Remote Sensing and Spatial Information Sciences, Volume XLVIII-2/W7-2024 Optical 3D Metrology (O3DM), Brescia, Italy, 12–13 December 2024.

Abstract

Integrating optical metrology into steelmaking and metalworking processes faces challenges not only from harsh conditions but also from a limited understanding of metrology concepts. The literature often overlooks distinctions between different uncertainty sources. This paper proposes a model for the quantification of uncertainty in dimensional measurements of open-die forged components, addressing the different uncertainty sources related to the measurand variability, to the instrumental uncertainty and to the definitional uncertainty. Guidelines for their evaluation are provided, and two case-studies related to measurement of forged shafts are presented and discussed.

Keywords: open forge measurement; uncertainty analysis; data fusion

1. Introduction

2D and 3D optical measurement techniques offer significant advantages when measuring objects at temperatures exceeding 500 °C, particularly in processes like open-die forging [1], a method used to reduce large steel ingots or billets into smaller, semi-finished products. In this process, whose scheme is presented in Figure 1, one or two manipulators are used to position the workpiece between the upper and lower dies of the forging press.

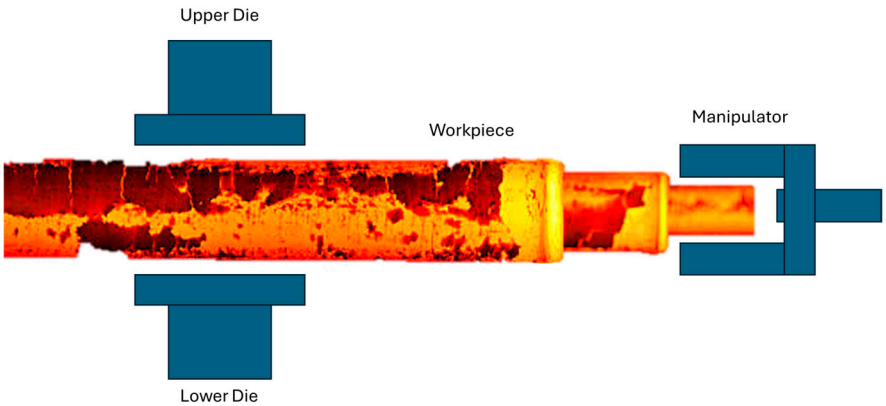

Figure 1. Scheme of open-die forging.

Unlike traditional die forging, which shapes the entire surface of the workpiece in one operation, open-die forging focuses on deforming localized sections of the material.

check for updates

Academic Editor: Ki-Nam Joo

Received: 5 April 2025
Revised: 16 July 2025
Accepted: 26 August 2025
Published: 2 September 2025

Citation: Tarabini, M. Uncertainty in Dimensional Measurements During Open-Die Forging. *Metrology* **2025**, *5*, 55. https://doi.org/10.3390/metrology5030055

As a result, the deformation process progressively alters the length and width of the workpiece while maintaining its overall volume [2]. Since the dimensions of the workpiece are typically on the scale of meters, accurate measurements helps in reducing the machining time, prevents parts from failing to meet specifications and minimize the energy waste [3].

In the majority of industries, dimensions of large open-die forged objects are still measured with contact measurement instruments by operators wearing special equipment to protect them from heat. The adoption of contactless measurement systems brings great advantages in terms of measurement uncertainty reduction.

Literature provides different examples of usage of Time of Flight (TOF), Laser Triangulation (LT), and Stereoscopic Systems (SS) with cameras in hot forging of bars [4]. Sections 1.1–1.4 outlines the literature reported in ref. [5]; Section 1.5 summarizes the measurement principles, measurement ranges and expected accuracy in the most relevant studies while Section 1.6 discusses the Reference Values and Uncertainty in the Existing Literature.

1.1. TOF Systems

TOF sensors offer accuracy in the order of a few mm in measuring distances over areas of several tens of meters, making them effective for capturing the general shape of forged components; in forging applications, TOF systems are based on single point, linear or 3D sensors that are moved by robots to scan the surface. Tian et al. [6] used a pulsed TOF laser rangefinder and a 2-DOF parallel-mechanical scanning device. During the measurement process, the coordinates of a target are determined through the continuous rotation of the scanner. The length dimension is obtained from two axial scans, which identify the positions of the two end faces of a cylinder. In a laboratory environment, the measurement discrepancies between the nominal value and the estimated value are approximately 2 mm for the diameter (ranging from 50 mm to 70 mm) and 4 mm for the length (ranging from 30 mm to 400 mm). He and colleagues [7] proposed a dual PRRR robotic system (where P and R represent prismatic and revolute joints, respectively) for measuring a hot cylindrical shell in a polar coordinate system. The system uses the circle matching method for measurement, positioning the rotating platform to ensure that the laser scanning plane is perpendicular to the cylindrical axis. The target object's coordinates are obtained by continuously rotating the laser sensor, with data conversion to the coordinate system performed using the Denavit-Hartenberg method. The measurement errors for diameter dimensions around 6 m were found to be less than 0.235%.

Other studies used commercial laser scanners acquire 3D geometries; in ref. [8], two Leica ScanStation2 TOF scanners allowed estimating the diameter of cylindrical components during forging. Accuracy was in the order of 8 mm when measuring diameters of more than 5 m. Researchers of Shanghai Heavy Machinery Factory Co. Ltd. (Shanghai, China) [9] designed a solution based on a linear sensor mounted on a servomotor for rotating the scanners during the acquisition. The scanning plane of the device is perpendicular to the main shaft of the motor, which can realize the 3D space measurement in the polar coordinate system; the dimensional error is less than 2%. The authors developed simulation software using a genetic algorithm to determine the position of the laser scanner and address the issue of scanner orientation. The acquisition process involves three scans, taken after rotating the object by 120°. The object is then separated from the background through 3D segmentation, and its shape is reconstructed using the Iterative Closest Point (ICP) algorithm. The measurement system was validated first on a cooled metal component and then on a hot cylindrical forged component during its shaping process. The results showed a discrepancy of less than 8 mm between the nominal and measured diameter values, for dimensions around 5 m.

Another work [10] proposed a system for dimensional measurements of complex annular forged components with free-form surfaces and a laser scanner. The system continuously acquires a point cloud of the object being measured during shaping, accounting for the changing position of the contour line over time. A Kalman time-sharing multiplexing particle filter method tracks noise and compensates for errors. Topological differential theory is used to identify a tangent cluster model and extract a surface. The measurement deviation of the reconstructed model from the nominal surface is less than 2.5 mm for pieces with a 600 mm radius.

Commercial products are also available: The company Minerals Technologies developed a system called La Cam Forge [11] based on range-finding technology. The laser system can be installed close to the forging process due to its protective cooling shell and is capable of measuring parameters such as linearity, straightness, and diameter of the object being measured.

1.2. Laser Triangulation

LT sensors provide distance or profiles with accuracy lower than 1 mm with standoff distances between the sensor and the forging usually in the order of 1 m. Lasers used for dimensional measurements during forging are typically blue or green due to better reflection and interaction with the material. Blue and Green wavelength are more effectively reflected and usually ensure a better scattering on uneven surfaces.

In simpler applications, single-point lasers are moved on a the surface by rotational joints during the rotational shaping phase [12]. In the specific case of cylindrical shells with the outer diameter of a shell of 6 m, the measurement error was lower than 6 mm. Other researchers [13] used a laser triangulation device to detect the diameter of hot forged cylinders. The research focused on the system calibration through the particle swarm optimization algorithm, to optimize the intrinsic and extrinsic calibration parameters of the camera. The calibration was performed by a rectangular block of a known size, and results showed an average error lower than 0.5 pixels. By moving the system along the main axis of the forging cylinder and rotating the cylinder itself, the contour of the object was obtained with an error lower than 1 mm for diameters of approximately 100 mm.

Han and colleagues [14] combined an industrial robot with a structured blue light 3D profilometer for scanning hot forgings in an industrial setting. An optical filter was used to avoid the influence of IR radiation emitted by the workpiece and a robot moved the scanner to obtain point clouds from different viewing angles. The scanning path was pre-designed for each specific workpiece and then executed automatically on the same shapes at high temperature. Experiments performed on objects at 900° showed that the alignment precision was 0.0013 rad and 0.28 mm. Other researchers [15] used a green laser with a wavelength of 530 nm for measuring the section of forged round shapes. The method consists of acquiring two images with and without the laser blade: the profile is derived by subtracting two images and post-processing the image with a median filter. The measurement uncertainty was lower than 1 mm for diameters of 100 mm.

A coordinate measuring system composed by eight laser profilometers manufactured by Zumbach, positioned in an octagonal arrangement has been proposed to capture the section profile of turbine blades [16]. The forging moves along the main axis of the turbine, and profilometers scan various sections; results evidenced an error range of 0.1 mm on a 700 mm turbine blade.

In addition to geometrical measurements, some works focused on machine learning to detect surface defects on measurements acquired by laser triangulation systems [17]. The application was based on the use of a striped laser with a wavelength of 405 nm and a camera, housed in cooled case. The algorithm looks for the center of mass peak by means

of morphological edge detection and median filtering. Then a Support Vector Machine recognized defects thanks to the training on a specific defect database.

1.3. Laser Scanners

A method for measuring the radial dimensions of ring parts during the forging process was proposed by Hu et al. [18]. This technique processes laser scanning data obtained from the outer radial section profile of ring forgings. Authors used a RIEGL VUX 1HA scanner for measuring rings with diameter of 300 mm. Point clouds were processed using multiple regression filtering algorithms; the declared measurement error varied between 0.1 and 1.3 mm for diameters between 260 and 270 mm.

1.4. Stereoscopic Systems

In hot forging, passive stereoscopic vision systems may offer advantages over TOF and LT systems. Passive SS are not affected by high reflectivity and emission from red-hot steel and are usually more affordable with respect to TOF and LT, although the accuracy is usually in the order of a few mm.

Li and colleagues [19] used a stereoscopic system to obtain the edges of prismatic forgings for a 3D reconstruction. The forged workpiece was identified by image segmentation and afterwards analyzed by observing the intensity in the red plane. The edges were interpolated by a Quadratic B-spline method; no errors were reported. Liu and colleagues [20] adopted an active stereoscopic system for hot forgings at different temperatures. The authors used a DLP projector (3M, PD80X) between two cameras. Under high temperatures, the profile of the light stripe becomes fringed and asymmetrical, reducing feature point extraction accuracy when fitted with a Gaussian profile. Authors proposed a modified asymmetrical Gaussian model to better describe the light stripe profile on hot cubic forgings. Laboratory tests showed a measurement error between 0.4 and 0.7% of the measure with diameters of approximately 140 mm. Liu and colleagues analyzed the effects of disturbances on the images quality and proposed a compensation strategy for the different environmental conditions [21]. Authors declared a measurement error 0.32 mm and a maximum relative error of 0.3% for cross-section dimensions in the order of 100 mm.

A multi-stereo active system was proposed by Jia et al. [22]; authors validated the system in laboratory and in a forging workshop obtaining a precision of up to 0.10% for prismatic bars with a side dimension between 1200 mm and 1500 mm, framed in scene of 8.6 m $\times$ 5.0 m.

Other researchers [23] proposed an active SS with a projected pattern for 3D reconstruction of forgings. Tests in forging environment reported a relative error of 0.79% for diameters in the order of 100 mm with a measurement time of 1.9 s. In another study [24] a measurement system with two perpendicular high-resolution cameras was used for measuring symmetric cylindrical forgings during a rotation. The method extracts the contour of the workpiece from four boundary curves obtained by detecting the edges of the forging. Authors created a 3D model to determine the total length along the main axis, the diameter, and the straightness of the piece. The experiments in a forging factory reported an error of up to 2% for the total length measurement in the order of 500 mm and 1% for the diameter estimation in the order of 50 mm.

More recently, Hurnik and colleagues [25] developed a new passive camera system that uses silhouettes in images to measure heavy cylindrical forgings. They introduced novel methods to improve the system's resilience to harsh industrial environments based on weighted edge filtering. The declared accuracy was 0.5 mm for axial measurements and 0.1 mm for diameter measurements within a 6 $\times$ 6 $\times$ 2 m volume. The same authors

proposed a multi camera method in which there was a decrease in measurement error proportional to the square root of the observation number [26]

1.5. Summary

Results presented in the previous sections are summarized in Table 1.

Table 1. Summary of the main literature review works.

Ref	Principle	Hardware Equipment	Technology	Error	Measure
[5]	TOF	Pulsed TOF laser rangefinder with 2-DOF parallel-mechanical scanning device	Continuous rotation scanning with axial scans	2 mm (D) 4 mm (L)	D: 50–70 mm L: 30–400 mm
[6]	TOF	Dual PRRR robotic system with laser sensor	Circle matching method with Denavit-Hartenberg transformation	<0.24%	6 m
[8]	TOF	Linear sensors mounted on a servomotor	Polar coordinate system with 3D segmentation and ICP algorithm	<2%	2–4 m
[7]	TOF	Two Leica ScanStation2 TOF scanners	Point Cloud registration during 120° rotation	8 mm	5.2 m
[9]	TOF	Laser scanner system	Kalman time-sharing multiplexing particle filter and topological differential theory	<2.5 mm	1200 mm
[10]	TOF	Range-finding laser system with protective cooling shell	Linear, straightness, and diameter measurement	Not reported	Not reported
[11]	LT	Single-point laser with rotational joints	Rotational shaping phase	<6 mm	6 m
[12]	LT	Laser triangulation device with particle swarm optimization for calibration	Moving system with contour acquisition	<1 mm	100 mm
[13]	LT	Industrial robot + structured blue light 3D profilometer with optical filter	Pre-designed scanning path with automated execution	0.28 mm	Not reported
[14]	LT	Green laser (530 nm) with image subtraction technique	Median filter for post-processing	<1 mm	100 mm
[15]	LT	Eight laser profilometers in octagonal arrangement	Moving system scanning turbine sections	0.1 mm	700 mm
[16]	LT	Striped laser (405 nm) + cooled camera	SVM-based defect detection	Not reported	Not reported
[18]	LS	RIEGL VUX 1HA	One-side observation, filtering data and interpolation	0.8 mm	D: 300 mm
[19]	SS (Passive)	Passive stereoscopic vision system	Quadratic B-spline method for edge interpolation	Not reported	Not reported
[20]	SS (Active)	DLP projector (3M, PD80X) between two cameras	Modified asymmetrical Gaussian model	0.4–0.7%	140 mm
[21]	SS (Active)	Compensation strategy for environmental conditions	Image compensation model	0.32 mm	122 mm
[22]	SS (Active)	Multi-stereo active system	Precision 3D reconstruction	0.10%	1200–1500 mm
[23]	SS (Active)	Active SS with projected pattern	Forging environment tests	0.79%	100 mm
[24]	SS (Passive)	Two perpendicular high-resolution cameras	Boundary curve extraction with 3D model creation	2% (L) 1% (D)	L: 500 mm D: 50 mm
[25,26]	SS (Passive)	Two or more high resolution cameras	Silhouette extraction with proprietary algorithms and fusion between multi cameras	0.5 mm	6 × 6 × 2 m

1.6. Reference Values and Uncertainty in the Existing Literature

The literature review highlights the general use of optical techniques for determining the geometrical characteristics of open die forged components, with measurement errors typically assessed by comparing the proposed systems against recognized gold standards. Bokhabirne and colleagues derived the metrological performances by comparing the diam-

eter measured with the proposed laser scanner with the diameter measured using a contact method currently used in the company [8]. Other authors used metallic workpieces with known geometries [9] to validate the measurement system at room temperature.

Only a few works [4,15] analyzed the measurement uncertainty with an approach consistent with the ISO Guide to the expression of Uncertainty in measurements [27]. Bračun and colleagues showed the clear distinction between single point measuring uncertainty obtained at room temperature in laboratory conditions and the overall variability dimensional measurement on the forged part. The single point measurement uncertainty affects individual data points describing the surface profile; accuracy of the system is usually evaluated by measuring known dimension of a specimen, such as the radius, the diameter or a length, and its uncertainty is typically lower than the point accuracy due to the interpolation of the surface profile with circles, splines or lines.

Surface irregularities influence the perceived measurement accuracy since part of the measurand variability is attributed to the measurement system. Open die forged components show deviations from the ideal geometric shape, with cross-sections that are neither perfectly circular nor polygonal. Furthermore, the transitions between sections of varying dimensions are typically smooth and gradual rather than sharply defined, complicating the measurement of individual segment lengths L, as illustrated in Figure 2.

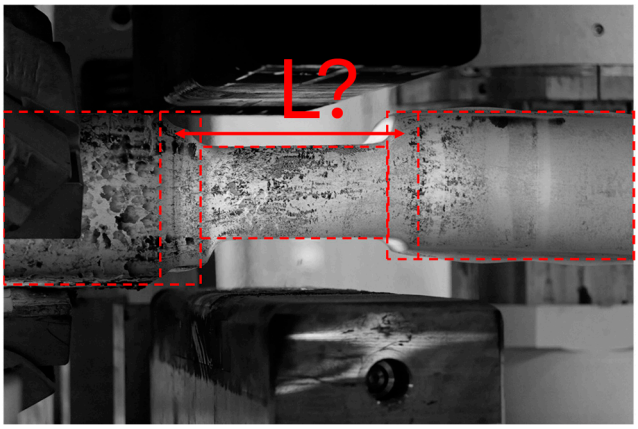

Figure 2. Example of a real contour of an open-die forged material. Dashed lines indicate the contour of an ideal workpiece composed by cylindrical parts and L is the unknown length of a cylindrical segment.

2. Method

A measurement model is a mathematical relationship linking the measured quantity (output Y) to the input quantities X influencing it. It generally takes the form:

$$Y = f(X_1, X_2, \ldots, X_j, \ldots X_m) \tag{1}$$

where

- Y is the measurand
- $X_1, X_2, \ldots, X_j, \ldots X_m$ are the input quantities contributing to the measurement result, including the desired input and the disturbances;
- f is a functional relationship between input and output, that may be linear or not.

The measurand, in the case of dimensional measurements, may be a diameter or a length of a part of the forged specimen, and is a function of the input quantities that are the dimensions of the specimen, the effect of environmental parameters such as the temperature of the object, and the characteristic of the measurement instrument.

The measurand is the idealized quantity we aim to measure (for instance the diameter of a perfect cylinder), while the real object deviates from this ideal shape due to imperfections like ovality, conicity, surface roughness, and geometrical changes due to the thermal expansion and surface oxidation. The measurement model bridges this gap by defining the measurand as a function of observable quantities, correction terms, and uncertainty sources. For example, the measured diameter may be expressed as the average of multiple readings across different orientations, with correction factors accounting for instrument lack of linearity and finite resolution, as well as shape deviations from the ideal one.

The model allows the measured value to approximate the ideal measurand, while the associated uncertainty quantifies the spread of possible true values. According to International Vocabulary of Metrology (VIM, [28]), uncertainty is the non-negative parameter characterizing the dispersion of the quantity values being attributed to a measurand, based on the information used. Uncertainty consists of multiple components that together form the overall uncertainty:

1. Measurand Variability, which reflects inherent fluctuations in the quantity being measured, including temporal changes influenced by uncontrollable factors.
2. Instrumental Uncertainty, summarizing errors originating from the measurement instruments, such as calibration inaccuracies, resolution, non-compensated nonlinear effects, and generic systematic and random error components.
3. Definitional Uncertainty, which arises from limitations in the definition of the measurand, and includes model approximations, methodological constraints, and assumptions.
4. Environmental Factors are sometimes included as a fourth source of measurement uncertainty; however, their influence can be incorporated into instrumental uncertainty (e.g., temperature effects on instrument behavior) and measurand variability (e.g., changes in the characteristics of the object being measured due to environmental conditions).

The overall measurement uncertainty u can be obtained by combining in quadrature the uncertainty components due to the measurand variability, to the instrument and the definitional uncertainty, u_{mv} u_i and u_{def} as:

$$u = \sqrt{u_{mv}^2 + u_i^2 + u_{def}^2} \tag{2}$$

According to the above-described measurement model, a diameter can be determined as:

$$D(T,t) = \frac{1}{n}\sum_{i=1}^{n}\left(M_i(t,T) + C_i\right) + \Delta_{def} \tag{3}$$

where

- D is a dimensional measurement.
- $M_i(t,T)$ are the direct readings of the measurement instrument at different temperatures T, taken at different time instants t.
- C_i are the correction factors compensating for systematic errors of the measurement system or disturbances (e.g., linearity, thermal expansion).
- Δ_{def} is the definitional uncertainty, according to the deviation between the physical model and the measurand.
- n is the number of measurement repetitions.

2.1. Measurand Variability

During forging processes, material properties vary over time; in some cases, these changes are small in comparison with other uncertainty sources and can be disregarded.

In steel forging, exposure to high temperatures in an oxygen-rich environment leads to oxidation, forming a surface layer known as scale. This oxide layer often detaches during forging, resulting in material loss that contributes to measurand variability and must be considered in the uncertainty evaluation.

Dimensions of the object being measured also depend on the temperature because of the material thermal expansion. As temperature T increases, the coefficient of thermal expansion of steel α generally rises as well: steel expands, on average, more at higher temperatures compared to lower ones, and the rate of expansion varies depending on the temperature range and the specific type of steel.

To account for these dependencies, the dimensional variation ΔD can be computed as a function of time and temperature as follows:

$$\Delta D(T,t) = D_0 \alpha(T)(T - T_0) - \Delta_{scale}(t,\ T) \tag{4}$$

where

- D_0 is the dimension of the object at room temperature T_0.
- $\alpha(T)$ is the temperature-dependent coefficient of linear expansion of the material.
- T is the instantaneous temperature of the forged material.
- $\Delta_{scale}(t,\ T)$ is the scale thickness formed and subsequently loss during the process at time t.

Since $\alpha(T)$, $\Delta_{scale}(t,\ T)$, T and t are affected by uncertainty, their contribution should be considered in the uncertainty budget. Uncertainty due to the measurand variability can be therefore computed using the partial derivative propagation as:

$$u_{mv}(T,t) = \sqrt{\sum_{j=1}^{n}\left[\left(\frac{\partial(\Delta D(T,t))}{\partial X_i}\right)u_{Xi}\right]^2} =$$

$$\sqrt{\left[\left(\frac{\partial(\Delta D(T,t))}{\partial D_0}\right)u_{D_0}\right]^2 + \left[\left(\frac{\partial(\Delta D(T,t))}{\partial \alpha}\right)u_{\alpha}\right]^2 + \left[\left(\frac{\partial(\Delta D(T,t))}{\partial T}\right)u_{T}\right]^2 + \left[\left(\frac{\partial(\Delta D(T,t))}{\partial \Delta_{scale}}\right)u_{\Delta_{scale}}\right]^2} \tag{5}$$

$$u_{mv}(T,t) = \sqrt{\left[\alpha(T)(T - T_0)u_{D_0}\right]^2 + \left[D_0(T - T_0)u_{\alpha}\right]^2 + \left[D_0\alpha(T)\ u_T\right]^2 + \left[u_{\Delta_{scale}}\right]^2}$$

At room temperature, α of steels ranges between 10 mm/(m°C) for ferritic stainless steels and 17 mm/(m°C) for austenitic stainless steel. Above 1000 °C, published data is limited [5], thus leading to larger uncertainties.

The scale thickness $\Delta_{scale}(t)$ depends significantly on temperature and time, but also on air humidity and the steel's chemical composition. In many companies, material loss due to scale is considered as a fixed percentage of the mass. In the literature, there is limited information. Δ_{scale} has been studied in the specific case of continuous casting of High-Strength Low-Alloy steel exposed to dry air and was 0.5 mm at 1100 °C after 30 min. At 1200 °C, Δ_{scale} increased to 0.75 mm over the same period [29].

2.2. Instrumental Uncertainty

Instrumental uncertainty should be assessed under conditions where all other uncertainty sources are either negligible or well-characterized. To account for environmental influences effectively, calibration shall be conducted in conditions that closely resemble the instrument's actual operating environment. The calibration can be performed at room temperature only if the instrument is insensitive to the temperature of the object being measured; otherwise, the interference of environmental effects such IR radiation may lead to an underestimation of the overall measurement uncertainty.

If the instrument behavior is temperature-dependent, performing calibration at high temperatures introduces challenges related to the oxidation of the reference specimen. A

potential solution is to use materials with low oxidation rates at high temperatures such as B445J1M stainless steel, which develops a scale thickness of less than 0.5 μm when exposed to air containing 18% water vapor at 1000 °C for 3 min. This minimal oxidation allows for the creation of disposable or recyclable calibration specimens. The calibration procedure may follow these steps:

1. Machine the specimen (e.g., via turning or milling) and measure it using a Coordinate Measuring Machine.
2. Heat the specimen to the desired temperature and promptly measure it with the instrument being calibrated to minimize oxidation effects.
3. After calibration, re-machining the surface, new measurement with Coordinate Measuring Machine and repeat the process as necessary.

This approach assumes minor deformation of the specimen due to residual stress; to minimize such deformations, appropriate heat treatments should be applied.

The uncertainty of the instrument U_i can be derived from the calibration and typically depends from the uncertainty associated with the reference specimen u_{ref}, from the instrument finite resolution, from the instrument repeatability, linearity over the measurement scale and data processing uncertainty sources (e.g., surface fitting).

Whenever the instrument is calibrated with n repeated measurements of a single reference specimen with uncertainty u_{ref}, u_i can be evaluated by combining the Type A uncertainty of the ISO GUM, u_A with other measurement uncertainty contributions related to the instrument u_{instr} such as the hysteresis, nonlinearity and the effect of the temperature of the forging on instrument performances, not accounted in u_A.

$$\begin{aligned} u_i &= \sqrt{(u_A)^2 + (u_{instr})^2 + \left(u_{ref}\right)^2} \\ &= \sqrt{\left(\frac{1}{\sqrt{n}}\sqrt{\frac{\sum_{i=1}^{n}(m_i - \overline{m})}{n-1}}\right)^2 + (u_{instr})^2 + \left(u_{ref}\right)^2} \end{aligned} \tag{6}$$

where

- n is the number of measurement repetitions.
- m_i is the i-th measurement.
- $\overline{m}$ is the arithmetic average of the n measurements.
- u_{ref} is the uncertainty of the reference specimen.
- u_{instr} instrumental contributions.

In case of instrumental calibration with different measurands, the uncertainty can be obtained by combining in quadrature u_{ref} and the root mean square of the residuals deriving from the regression of experimental data.

Numerical values of u_i obviously depend on the specific instrument, but the literature evidenced as typical values:

- u_i smaller than 1 mm for laser profilometers for high temperatures with full scales around 1 m
- u_i between 2 and 10 mm for passive stereoscopic systems with full-scale between 1 and a few m
- u_i larger than 10 mm for LIDARs with measuring ranges of several meters.

2.3. Definitional Uncertainty

In dimensional measurements, the definitional uncertainty quantifies the difference between a nominal parameter (for instance, the diameter) and the real object. According to the VIM, the measurand should be defined in such a manner that the related definitional

uncertainty is considerably lower than the target uncertainty. This implies that in order to reduce the overall measurement uncertainty on forged materials, it is essential to employ complex geometric models accounting for measurand non-idealities.

Once it is established that the measurand is represented with a model with finite detail, it is clear that the associated definitional uncertainty can be improved by the adoption of more refined models. By increasing the complexity and fidelity of the mathematical model used in a measurement, a portion of what might otherwise be treated as random error can be systematically accounted for. The measurement model is conceptually described by Equation (1); in the specific case of coordinate metrology, point clouds are interpolated with fitting curves or surfaces to compare the real workpiece with technical drawings. f is therefore the equation of the least-square fitting curve and X_i are the coordinate of the sampled points. After the model is fitted to the measurement data, the differences between the individual observed points and the values predicted by the model (residual) obviously depend on the model complexity.

An illustrative example of the effect of the order of polynomial regression is shown in Figure 3. Part (a) shows simulated data, while parts (b) and (c) show the residuals of the regression. The adoption of a linear model, in this case, is an example of underfitting. The simulated data inherently exhibit a parabolic trend and the linear regressor is too simplistic; the model inadequacy is evidenced by the residuals (which have a parabolic trend) and by their large values.

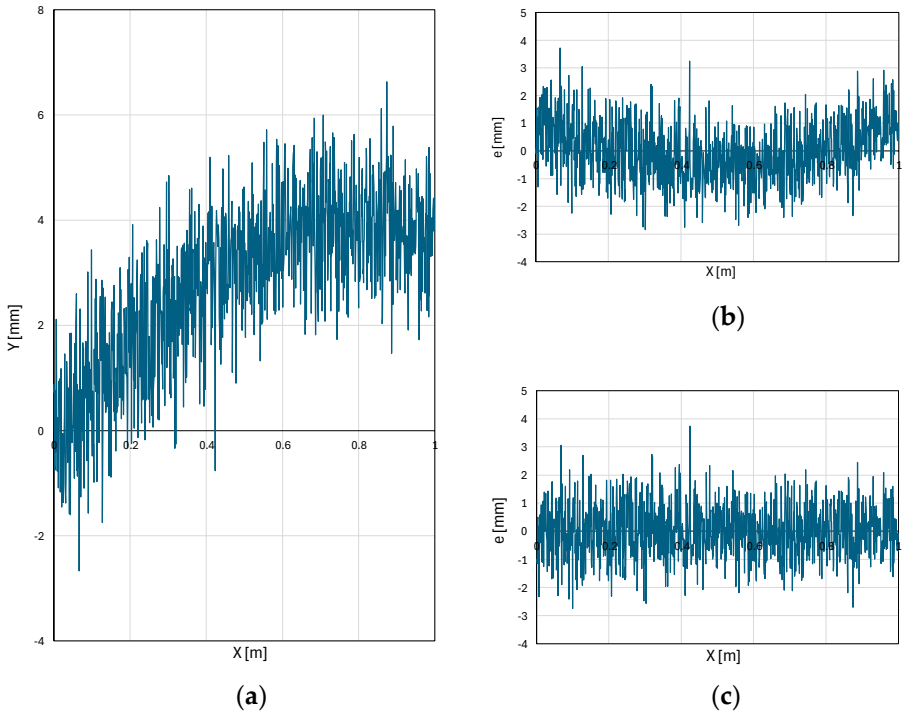

Figure 3. Point coordinates (**a**) and residuals obtained with a linear (**b**) and quadratic (**c**) fits.

By adopting a quadratic model, the complexity of the model is increased to better match the inherent nature of the data. Residuals (part (c)) do not exhibit a clear pattern and their values are reduced. Continuing to increase the order of the polynomial can lead to overfitting: models are overly complex and begin to fit the random noise in the data, rather than the geometrical data themselves.

Definitional uncertainty arises because there is an inherent ambiguity in the application of the geometrical model to the real-world data. The least-squares fitting minimizes the residuals to find one specific solution, which however, is just one of many possible

interpretations of the real phenomenon. Residuals are the tangible evidence and the direct cause of definitional uncertainty, and the magnitude and distribution of the residuals show how imperfect the model is.

Whenever the definitional uncertainty is dominant, comparing measurements from different instruments can be misleading. Many studies overlook this factor, mistakenly mixing instrumental effects with definitional uncertainty.

3. Case-Study

Uncertainty has been evaluated in two examples. In the first one a 2D laser scanner has been used to measure the diameter of forged bars, while in the second one a 2D camera has been used to detect the diameter of similar bars by detecting the silhouette.

3.1. Laser Triangulation

3.1.1. Instrumental Uncertainty

The laser DSE O2DS underwent a metrological characterization procedure that included repeatability on flat and circular surfaces; results are reported in ref. [5]. The standard deviation of repeatability u_A varied between 0.3 and 0.5 mm on flat surfaces and between 0.4 and 0.6 mm on cylinders. The uncertainty of the reference system u_{ref} was 0.1 mm for the linear surfaces and 0.2 mm for the diameters. Instrumental uncertainty U_{instr} included a systematic diameter overestimation of 0.8 mm (only in presence of circular profiles) and an effect of nonlinearity lower than 0.2 mm. The effect of temperature of the forging on instrumental uncertainty is negligible: the optical sensor is cooled by water and compressed air, and the blue laser diode with wavelength between 440 and 450 nm, ensuring reliable measurement until 2000 °C according to the manufacturer declared performances.

The (standard) instrumental uncertainty was evaluated according to Equation (6) and is 0.55 mm for flat surfaces and 1 mm for circular surfaces, as summarized in Table 2; values are expressed as standard uncertainties; expanded uncertainty (with confidence intervals of 95 or 99.7%) can be computed by estimating the residual degrees of freedom using the Welch-Satterthwaite formula and by using the percentiles of the T-Student distribution. Values are compatible with those declared by the manufacturer (resolution, radial and polar reproducibility 0.7 mm, linearity of 1.4 mm).

Table 2. Summary of standard instrumental uncertainty sources.

Measurand	u_A [mm]	u_{ref} [mm]	u_{instr} [mm]	u_i [mm]
Bar	0.50	0.10	0.20	0.55
Cylinder	0.60	0.18	0.82	1.0

3.1.2. Measurand Variability

The measurand variability has been estimated in the specific case of a forged cylindrical bar with nominal diameter L_0 of 820 mm, with an uncertainty of 5 mm. The steel coefficient of thermal expansion declared by the foundry was 12 mm/(m°C) at room temperature and between 14 and 16 mm/(m°C) at the forging temperature, i.e., between 1150 °C and at 1000 °C. Assuming a maximum error of $\alpha(T)$ of 2 mm/(m°C) and a uniform error distribution, the standard uncertainty of $\alpha(T)$ obtained by dividing the maximum error by $2\sqrt{3}$ is 0.6 mm/(m°C).

The temperature was controlled by a pyrometer; temperature uncertainty deriving from instrumental effects and from lack of information about the high-temperature emis-

sivity has been estimated with dedicated tests on the production plant and is 15 °C. The temperature at the end of the forging process was 1000 °C.

The scale thickness was estimated by the blacksmith with an empirical equation derived from experiments performed on specific classes of steel.

$$\Delta_{scale} = k\sqrt{t} \tag{7}$$

where t is the time in minutes and k is a coefficient between 0.1 and 0.5 mm/s$^{0.5}$ as a function of temperature (higher values corresponding to higher temperature). Figure 4 illustrates the trend of scale thickness in relation to changes in oxidation time and the coefficient k.

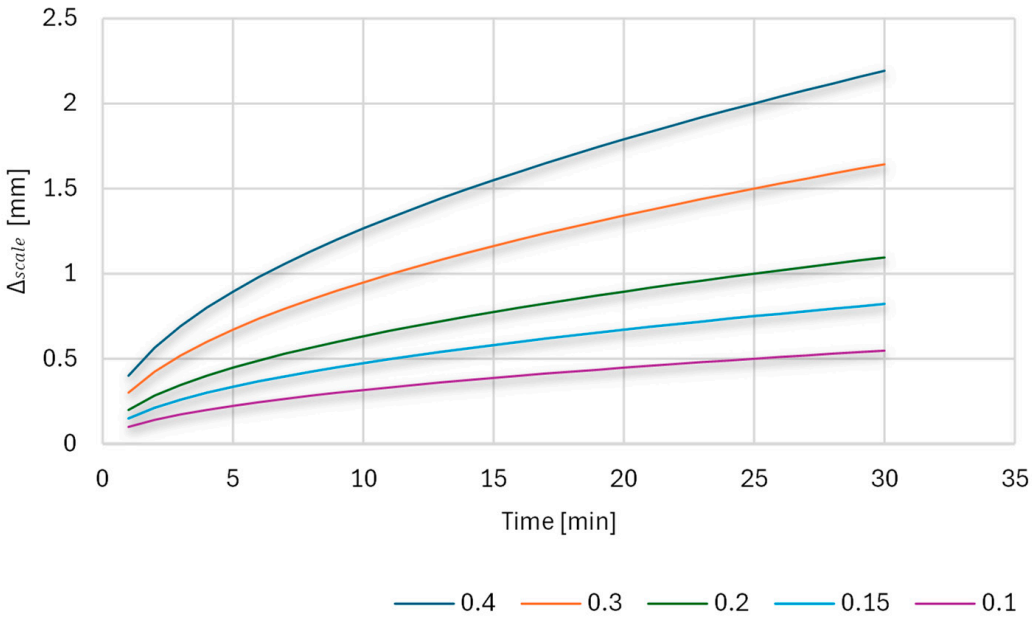

Figure 4. Estimation of the scale thickness Δ_{scale} as a function of the coefficient k (curves of different colors in the plot).

Δ_{scale} cannot be treated as a systematic component, and it is more cautious to consider, given the estimated duration of the forging and the expected temperature, the maximum gap between curves of Figure 3, thus obtaining, after 20 min, a maximum error of 1.8 mm, corresponding to a standard uncertainty of 0.5 mm.

$u_{mv}(T, t)$ can be computed according to Equation (5), and in this specific case is 0.7 mm.

3.1.3. Definitional Uncertainty

Figure 5 shows the difference between the fitted geometry and the approximation errors of point clouds acquired by a laser triangulation system on a cylindrical forged shaft with diameter of 0.5 m.

The circular fit led to the identification of a diameter of 496 mm and an RMS of the residual of 4 mm. The adoption of an elliptical model (accounting for ovality) led to the identification of a major axis of 506 mm and a minor axis of 486 mm; residuals reduced to 1.8 mm.

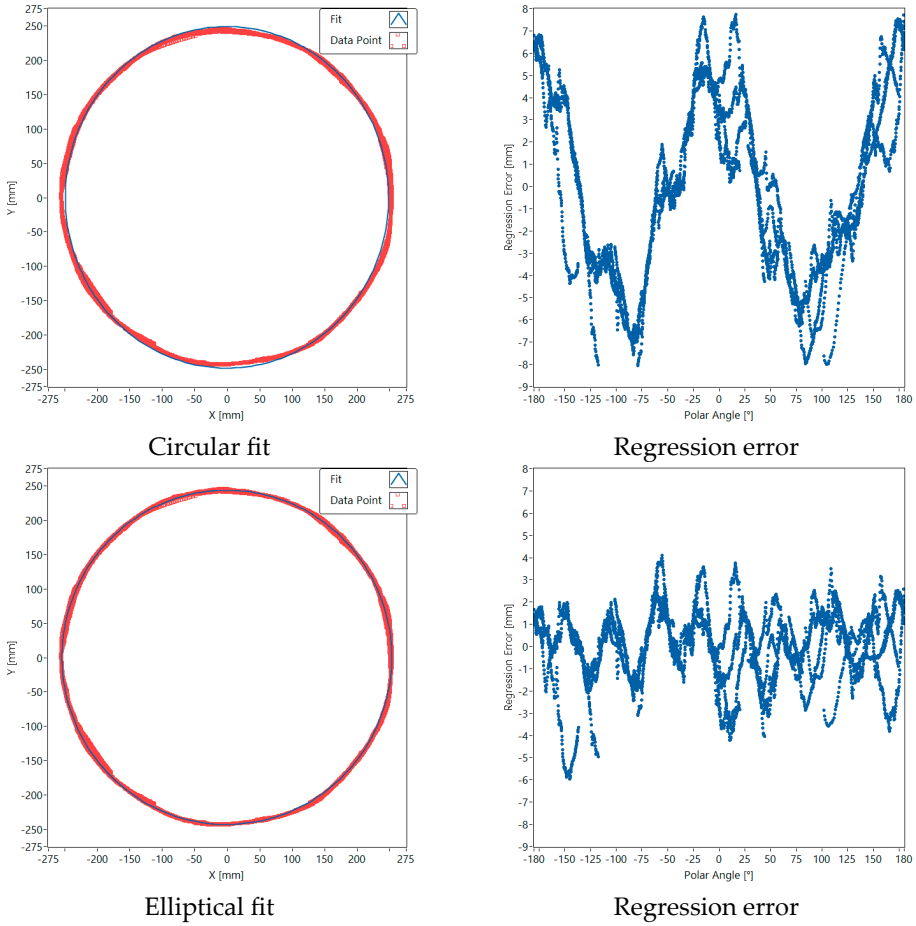

Figure 5. Comparison between the reconstruction of a real forged geometry with a circular model or with an elliptical model and resulting regression errors (right column).

3.1.4. Comparison Between Uncertainty Sources

In this case, the instrumental uncertainty was 1 mm, while uncertainty due to the thermal effects was 0.7 mm. The definitional uncertainty due to the adoption of a circular model in presence of specimen ovality was 4 mm. In these conditions, the overall measurement uncertainty obtained from Equation (2) is 4.2 mm and is governed by definitional uncertainty. The adoption of an elliptical model reduced the overall uncertainty to 2.2 mm.

3.2. Two-Dimensional Camera

An RGB Camera manufactured by IDS GMBH with resolution of 1936 × 1096 px was equipped with a CHIO lens with focal distance of 12 mm. A MidOpt filter with central wavelength of 635 nm was used to ease the detection of the edges of the forged bar at the forging temperature, reducing the interference with other light sources. The camera was positioned to obtain a resolution of approximately 3 mm/px in order to frame the entire shaft geometry and was calibrated by positioning a checkerboard with a dimension of 1 × 0.7 m on the center of the forge.

3.2.1. Instrumental Uncertainty

Repeatability tests were performed in laboratory conditions by acquiring the silhouette of machined cylinders with diameter of 125 mm with random background. The cylinder was positioned to ensure the same Field of View of the operative conditions.

Since the systematic error components are compensated by the checkerboard calibration performed on the plane of the cylinder axis, and since the residual reprojection error after the geometric compensation described in refs. [30,31] was small in comparison with

the uncertainty introduced by the edge detection algorithms, instrumental uncertainty can be quantified by the standard deviation of repeatability u_A, that was 0.4 mm. Assuming an optimization of the camera position with respect to the specimen in order to optimize the framed scene, uncertainty can be expressed as 0.3 % of the measured diameter.

3.2.2. Measurand Variability

The measurand variability can be assumed equal to the one studied in Section 3.1.2, since the steel characteristics are the same.

3.2.3. Definitional Uncertainty

Since the real geometry of the workpiece is approximated with a cylinder, the definitional uncertainty has been evaluated by computing the silhouette of the cylinder as shown in Figure 6.

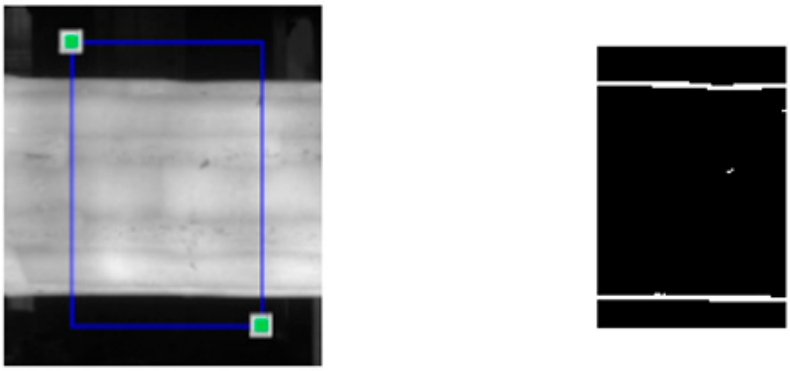

Image of the profile Profile edges

Figure 6. Silhouette of the forged bar and profiles detected with fit-to-purpose algorithms.

The diameter was computed by converting the average distance between the upper and lower edges into physical coordinates and compensating for the perspective distortion using the approach defined in ref. [30,31]. Since upper and lower edges were not linear and parallel, the minimum, average and maximum distances D_{min}, D_{mean}, and D_{max} were computed. The type B uncertainty associated with the diameter measurement was used to quantify the definitional uncertainty U_{def}. The range (D_{max}–D_{min}) was therefore divided by $\sqrt{12}$, assuming a uniform distribution of values within the range.

Twelve forged bars with D_{cal} between 650 and 1150 mm were measured. Figure 7 compares U_{def} with the instrumental uncertainty identified in Section 3.2.1.

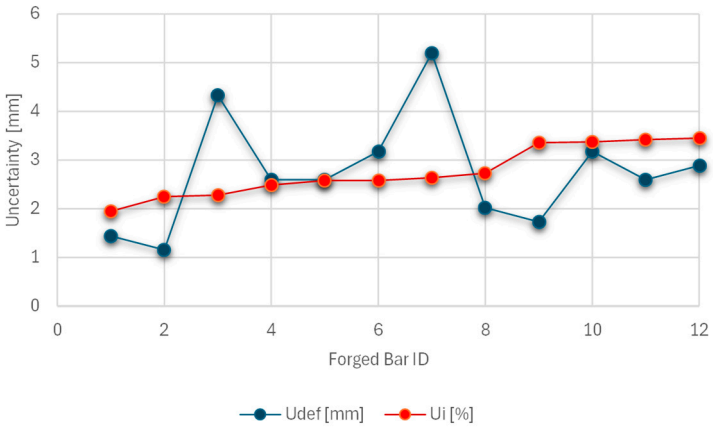

Figure 7. Comparison between the definitional and instrumental uncertainty in different measurements in measurements of 12 different forged bars.

3.2.4. Comparison Between Uncertainty Sources

The instrumental uncertainty ranged between 2 and 4 mm depending on the diameter of the forged bar dimensions, while the uncertainty related with thermal effects were quantified in 0.7 mm. The definitional uncertainty varied between 1 and 5 mm depending on the specimen. The overall uncertainty can be computed as per Equation (2), combining the instrumental uncertainty and the definitional uncertainty presented in Figure 7 with the definitional uncertainty related with thermal effects.

The overall measurement uncertainty, shown in Figure 8, varies between 2.5 and 6 mm. On average, it is due to an equivalent contribution of instrumental effects and of definitional uncertainty.

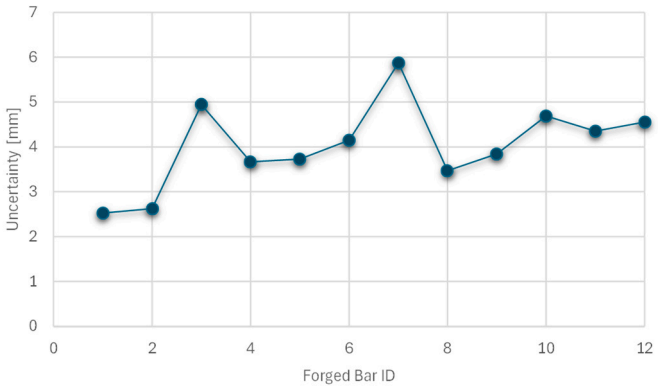

Figure 8. Overall measurement uncertainty in 12 different forged bars.

4. Discussion

4.1. Uncertainty Model

The proposed framework for the evaluation of measurement uncertainty in steel forging allows us to overcome the overly simplistic focus on instrumental uncertainty widely adopted in the literature. The model equally considers measurand variability, instrumental uncertainty, and definitional uncertainty. The analysis on the two case-studies demonstrated that not accounting for any of these components, particularly the latter two, can lead to a significant underestimation of the total uncertainty and, consequently, to poor process control.

A key implication of our model is the understanding that the workpiece changes its shape due to thermal contraction and scale formation/loss and that the measurand variability is a significant component of overall uncertainty. Critical parameters, such as the temperature-dependent coefficient of thermal expansion and scale thickness, are poorly documented in existing literature for typical forging conditions. Consequently, current manufacturing tolerances are oversized to compensate for these unknown contributions.

The second component is instrumental uncertainty: in scientific literature, room-temperature tests are often used to quantify the instrument repeatability, which is supposed to be coincident with the measurement uncertainty. The proposed high-temperature calibration procedure, while complex, is essential for quantifying how instruments perform under operational conditions. The comparison between different technologies—such as optical systems and contact sensors—becomes meaningful only when properly dealing with all the uncertainty components.

Another critical factor is definitional uncertainty. The definitional uncertainty is not a minor error source, but a fundamental limit imposed by the mismatch between an ideal geometric model and a physically imperfect workpiece. This is especially true in the early stages of forging, where the material's shape is rough and deviates significantly from any simple geometric primitive. The choice of the fitting model is not a simple data processing

step, but a critical decision that defines what is being measured and sets a floor on the achievable uncertainty.

The uncertainty model allows describing the shifting dominance of the three uncertainty components throughout the forging process.

- In the initial, rough shaping stages, measurand variability (due to high temperatures and rapid scaling) and definitional uncertainty (due to irregular shapes) dominate the overall uncertainty.
- In the final finishing stages, as the workpiece approaches its target geometry and temperature stabilizes, instrumental uncertainty may become the more significant contributor, but it is often smaller than the other two causes.

This dynamic perspective implies a process-aware metrology strategy, where the uncertainty budget is evolving during each specific stage of production.

4.2. Case Studies

The two case studies provided practical examples for the application of the proposed theoretical framework, showing the relative importance of different uncertainty sources based on the chosen technology and the specific workpiece characteristics. The laser triangulation example (Section 3.1) showed how definitional uncertainty can be the dominating component in forging: the use of an overly simplistic circular model for an irregularly shaped workpiece resulted in a dominant definitional uncertainty of 4 mm. This finding shows, for instance, which investing in a more precise instrument would have been useless without focusing on a more complex geometric model, that however requires more complex measurement procedure and data processing approaches.

In contrast, the 2D camera case study (Section 3.2) presents a more balanced scenario where instrumental and definitional uncertainties make comparable contributions to the overall budget. Here, the instrumental uncertainty was inherently larger due to the system's lower resolution, while the definitional uncertainty varied significantly with the geometric irregularities of each forged bar. This highlights a different but equally important takeaway: in applications like this, reducing the overall measurement uncertainty requires both hardware improvements (e.g., a higher resolution camera or optimized positioning) and/or software enhancements (e.g., more robust edge detection and analysis).

The two examples evidence that a preliminary analysis is always necessary to identify the dominant uncertainty source for a given application, ensuring that resources and engineering efforts are directed where they will have the most impact.

4.3. Practical Guidelines

The evaluation of the overall uncertainty requires a structured procedure to separately quantify the three uncertainty components.

The measurand variability is mostly related to the effects of temperature, which can be compensated by measuring the forged material's temperature and by knowing the real material's coefficient of thermal expansion. Oxidation effects should be estimated accounting for the thickness of the scale formed during forging and its impact on the measured dimension.

Instrumental uncertainty requires a systematic approach involving calibration procedures conducted under conditions that closely resemble the actual operating environment. The calibration can be performed at room temperature if the instrument has been designed to be insensitive to the temperature of the object being measured. Since calibration at high temperatures introduces challenges related to oxidation of the reference specimen, materials with low oxidation rates are recommended. The calibration process should include machining and measuring a reference specimen using a CMM, followed by heat-

ing the specimen to the desired temperature and measuring it again with the instrument being calibrated.

Definitional uncertainty, although inherently complex, can be estimated by acquiring una tantum a 3D point cloud of the workpiece at a suitable stage in the forging process. This point cloud can serve as a reference to quantify deviations from the ideal design.

4.4. Future Works

Future research should focus on further refining the measurement models and exploring advanced techniques for reducing definitional uncertainty. This involves using 3D point cloud data to better capture the true dimensions of forged components. Oxidation models can help in predicting the material waste due to oxidation and therefore reducing the metal allowance, which may exceed 10% of the ingot mass in complex shaping operations. Since the cost of the forge is related to the heating of the material, great environmental benefits could derive from process optimization.

5. Conclusions

This work proposed a framework for the quantification of uncertainty in steel forging. The model incorporates factors beyond instrumental error and integrates three components, which are the instrumental uncertainty, the measurand variability, and the definitional uncertainty. Two case studies confirmed the model and evidenced that inadequate geometric model may produce a definitional uncertainty larger than other error sources, making instrument precision a secondary factor.

The conclusion is that no single source of uncertainty is dominant. Uncertainty depends on the measurement technology and on the workpiece condition. Therefore, an effective industrial metrology strategy must first identify the largest contributor to the uncertainty budget. This targeted approach ensures that engineering efforts result in improved process control.

Funding: This research received no external funding.

Data Availability Statement: Data available on request due to restrictions.

Acknowledgments: The author gratefully acknowledges the support from One-Off Solution and FOMAS for the research in this field. Special thanks are also extended to Silvia Barella, Renato Casartelli, Stefano Parma and Stefano Borroni for their valuable suggestions on practical aspects related to metallurgy, steel oxidation and applicability of measurement processes in real industrial settings.

Conflicts of Interest: The author declares no conflicts of interest.

Abbreviations

The following abbreviations are used in this manuscript:

U	Uncertainty
TOF	Time of Flight
LIDAR	Light Detector and Ranging
GUM	Guide to the expression of Uncertainty in Measurements
VIM	International Vocabulary of Metrology
RMS	Root Mean Square

References

1. Dudra, S.P.; Im, Y.T. Investigation of metal flow in open-die forging with different die and billet geometries. *J. Mater. Process Technol.* **1990**, *21*, 143–154. [CrossRef]

2. Nye, T.J.; Elbadan, A.M.; Bone, G.M. Real-Time Process Characterization of Open Die Forging for Adaptive Control. *J. Eng. Mater. Technol.* **2001**, *123*, 511–516. [CrossRef]
3. Zhang, Y.C.; Han, J.X.; Fu, X.B.; Zhang, F.L. Measurement and control technology of the size for large hot forgings. *Measurement* **2014**, *49*, 52–59. [CrossRef]
4. Ghiotti, A.; Schöch, A.; Salvadori, A.; Carmignato, S.; Savio, E. Enhancing the accuracy of high-speed laser triangulation measurement of freeform parts at elevated temperature. *CIRP Ann.* **2015**, *64*, 499–502. [CrossRef]
5. Tarabini, M. Red Hot Steel: Challenges of 3D Optical Metrology in Open-Die Forging. *Int. Arch. Photogramm. Remote Sens. Spatial Inf. Sci.* **2024**, *XLVIII-2/W*, 169–175. [CrossRef]
6. Tian, Z.; Gao, F.; Jin, Z.; Zhao, X. Dimension measurement of hot large forgings with a novel time-of-flight system. *Int. J. Adv. Manuf. Technol.* **2009**, *44*, 125–132. [CrossRef]
7. He, J.; Gao, F.; Wu, S.; Liu, R.; Zhao, X. Measure dimension of rotating large hot steel shell using pulse laser on PRRR robot. *Measurement* **2012**, *45*, 1814–1823. [CrossRef]
8. Bokhabrine, Y.; Seulin, R.; Voon, L.F.C.L.Y.; Gorria, P.; Girardin, G.; Gomez, M.; Jobard, D. 3D characterization of hot metallic shells during industrial forging. *Mach. Vis. Appl.* **2012**, *23*, 417–425. [CrossRef]
9. Du, Z.; Wu, Z.; Yang, J. 3D measuring and segmentation method for hot heavy forging. *Measurement* **2016**, *85*, 43–53. [CrossRef]
10. Kong, T.; Zhang, Y.; Fu, X. The model of feature extraction for free-form surface based on topological transformation. *Appl. Math. Model.* **2018**, *64*, 386–397. [CrossRef]
11. Home | Minerals Technologies Inc. Available online: https://www.mineralstech.com/ (accessed on 15 July 2024).
12. Fu, X.; Zhang, Y.; Tao, K.; Li, S. The outer diameter detection and experiment of the circular forging using laser scanner. *Optik* **2017**, *128*, 281–291. [CrossRef]
13. Zhang, Y.C.; Han, J.X.; Fu, X.B.; Lin, H.B. An online measurement method based on line laser scanning for large forgings. *Int. J. Adv. Manuf. Technol.* **2014**, *70*, 439–448. [CrossRef]
14. Han, L.; Li, Z.; Zhong, K.; Yi, J.; Shi, Y.; Cheng, X.; Zhan, G.; Chen, R.; Beyerer, J.; León, F.P. Automatic 3D inspection metrology for high-temperature objects. In *Automated Visual Inspection and Machine*, 2nd ed.; SPIE Optical Metrology: Munich, Germany, 2017; Volume 10334, pp. 174–182. [CrossRef]
15. Bračun, D.; Škulj, G.; Kadiš, M. Spectral selective and difference imaging laser triangulation measurement system for on line measurement of large hot workpieces in precision open die forging. *Int. J. Adv. Manuf. Technol.* **2017**, *90*, 917–926. [CrossRef]
16. Schöch, A.; Savio, E. High-Speed Measurement of Complex Shaped Parts by Laser Triangulation for In-line Inspection. In *Metrology*; Springer: Berlin/Heidelberg, Germany, 2019; pp. 1–22. [CrossRef]
17. Veitch-Michaelis, J.; Tao, Y.; Walton, D.; Muller, J.-P.; Crutchley, B.; Storey, J.; Paterson, C.; Chown, A. Crack detection in 'as-cast' steel using laser triangulation and machine learning. In Proceedings of the 2016 13th Conference on Computer and Robot Vision, CRV 2016, Victoria, BC, Canada, 1–3 June 2016; pp. 342–349. [CrossRef]
18. Lu, Z.; Zhou, Q.; Zhang, Y. Dimension measurement method of ring forgings based on laser scanning and multiple regression filtering algorithm. *Meas. Sci. Technol.* **2023**, *34*, 105017. [CrossRef]
19. Li, Z.; Xia, Q.; Pan, Y.; Wu, Z. Internal Contour Extraction Algorithm Based on Quadratic B-spline for Images of Hot Long Shaft Forgings. *Adv. Mat. Res.* **2012**, *472–475*, 2274–2278. [CrossRef]
20. Liu, W.; Jia, Z.; Wang, F.; Ma, X.; Wang, W.; Jia, X.; Song, D. An improved online dimensional measurement method of large hot cylindrical forging. *Measurement* **2012**, *45*, 2041–2051. [CrossRef]
21. Liu, Y.; Jia, Z.; Liu, W.; Wang, L.; Fan, C.; Xu, P.; Yang, J.; Zhao, K. An improved image acquisition method for measuring hot forgings using machine vision. *Sens. Actuators A Phys.* **2016**, *238*, 369–378. [CrossRef]
22. Jia, Z.; Wang, L.; Liu, W.; Yang, J.; Liu, Y.; Fan, C.; Zhao, K. A field measurement method for large objects based on a multi-view stereo vision system. *Sens. Actuators A Phys.* **2015**, *234*, 120–132. [CrossRef]
23. Zhou, Y.; Wu, Y.; Luo, C. A fast dimensional measurement method for large hot forgings based on line reconstruction. *Int. J. Adv. Manuf. Technol.* **2018**, *99*, 1713–1724. [CrossRef]
24. Zatočilová, A.; Paloušek, D.; Brandejs, J. Image-based measurement of the dimensions and of the axis straightness of hot forgings. *Measurement* **2016**, *94*, 254–264. [CrossRef]
25. Hurník, J.; Zatočilová, A.; Koutný, D.; Paloušek, D. Enhancing the accuracy of forging measurement using silhouettes in images. *Measurement* **2022**, *194*, 111059. [CrossRef]
26. Hurník, J.; Zatočilová, A.; Konečná, T.; Štarha, P.; Koutný, D. Multi-view camera system for measurement of heavy forgings. *Int. J. Adv. Manuf. Technol.* **2022**, *121*, 7295–7310. [CrossRef]
27. *ISO/IEC Guide 98-1:2024*; Guide to the Expression of Uncertainty in Measurement—Part 1: Introduction. International Organization for Standardization: Geneva, Switzerland, 2024. Available online: https://www.iso.org/standard/82708.html (accessed on 26 March 2025).

28. *ISO/IEC Guide 99:2007(en)*; International Vocabulary of Metrology—Basic and General Concepts and Associated Terms (VIM). International Organization for Standardization: Geneva, Switzerland, 2007. Available online: https://www.iso.org/obp/ui/es/#iso:std:iso-iec:guide:99:ed-1:v2:en (accessed on 26 March 2025).
29. Huitron, R.M.P.; López, P.E.R.; Vuorinen, E.; Jalali, P.N.; Pelcastre, L.; Kärkkäinen, M. Metals Scale Formation on HSLA Steel during Continuous Casting Part I: The Effect of Temperature-Time on Oxidation Kinetics. *Metals* **2020**, *10*, 1243. [CrossRef]
30. Marcotuli, V. A Contactless Measurement System for High Temperature Shaft Manufacturing in Open Die Forging. 2023. Available online: https://www.politesi.polimi.it/handle/10589/188973 (accessed on 26 June 2025).
31. Marcotuli, V.; Lal, N.; Scaccabarozzi, D.; Tarabini, M. A Vision-based Measurement System for Semi-Finished Cylindrical Geometries. In Proceedings of the 2020 IEEE International Workshop on Metrology for Industry 4.0 and IoT, MetroInd 4.0 and IoT, Rome, Italy, 3–5 June 2020; pp. 288–292. [CrossRef]